Special Collection of Papers

This article is dedicated to Professor Satoshi Ōmura in celebration of his 2015 Nobel Prize.

Regular Article

Design, Synthesis and Biological Evaluation of a Structurally Simplified Syringolin A Analogues

Takuya Chiba,[a] Shun Kitahata,[a] Akira Matsuda,[a,b] and Satoshi Ichikawa*[,a,b]

[a] *Faculty of Pharmaceutical Science, Hokkaido University; Kita-12, Nishi-6, Kita-ku, Sapporo 060–0812, Japan: and* [b] *Center for Research and Education on Drug Discovery, Faculty of Pharmaceutical Science, Hokkaido University; Kita-12, Nishi-6, Kita-ku, Sapporo 060–0812, Japan.*

Received February 24, 2016; accepted March 13, 2016

In this study, we designed and synthesized a structurally simplified syringolin A analogue 4, which could have a switched hydrogen bonding interaction with the *β*5 subunit of 20S proteasome. This analogue exhibits potent *β*5 proteasome inhibitory activity with an IC_{50} value of 107 nM. It also shows cytotoxicity against a range of human cancer cells at submicromolar level (109–254 nM). This analogue is expected to be a lead compound as a next generation proteasome inhibitor because of its simple structure.

Key words proteasome; natural product; anticancer

Multiple myeloma is a hematological malignancy, where clonogenic mature plasma cells accumulate in bone marrow. These malignant cells multiply rapidly and interfere with the production of normal blood cells in bone marrow, and produce abnormal monoclonal immunoglobulins called M proteins in large amount. Bortezomib (Velcade®)[1] and carfilzomib (Kyprolis®)[2] have been approved by U.S. Food and Drug Administration (FDA) for the treatment of multiple myeloma. They are inhibitors of proteasome,[3] which is a complex machinery composed of many subunits. Amongst these subunits, *β*1, *β*2, and *β*5 subunits have caspase-like, trypsin-like and chymotrypsin-like catalytic activities, respectively. Proteasome degrades ubiquitin-labeled proteins, and is responsible for the maintenance of an intracellular protein expression.[4] Inhibition of proteasome results in accumulation of unnecessary proteins that ultimately causes cell death. Bortezomib reversibly inhibits proteasome to cause apoptosis of malignant plasma cells. The clinical introduction of bortezomib has changed the treatment paradigm of multiple myeloma resulting prolonged survival of patients. However, there are some drawbacks in clinical use of bortezomib such as peripheral neuropathy as well as drug resistance, which is a common issue to be concerned in cancer chemotherapy.[4–6] Although several proteasome inhibitors are currently under clinical trials,[3] new proteasome inhibitors are still necessary to be developed.

Syringolin A (**1**, Fig. 1) is a naturally occurring 12-membered macrolactam isolated from a strain of the plant pathogen *Pseudomonas syringae* pv. *syringae* in 1998.[7] It irreversibly inhibits proteasome by a 1,4-addition of the hydroxyl group of the N-terminal threonine (Thr) residue on the *β*5 subunit to the *α*,*β*-unsaturated carboxamide moiety embedded in **1**.[8] Since the mode of inhibition of **1** is different from that of bortezomib and carfilzomib, **1** is expected to be a new lead as an anti-multiple myeloma drug. The fact that **1** can exhibit a moderate *β*5 subunit inhibitory activity (K_i' value of 0.8 μM for *β*5) along with high cytotoxicity (IC_{50} value of 8.5 μM for human myeloma MM1.S cells) has motivated several groups to improve its biological activity.[9–13] The X-ray crystal structure of the yeast 20S proteasome covalently bound to **1** (PDB code: 2ZCY) has been elucidated.[8] The structure indicates that in the *β*5-subunit, the isopropyl side chain directly attached to the 12-membered ring of **1** is recognized by an S1 subsite and that of the internal valine (Val) residue was recognized by an S3 subsite, which constitutes a hydrophobic pocket that can accept a larger hydrophobic substituent than the isopropyl group (Fig. 2). Moreover, a hydrogen bonding between the NH of the internal Val residue and the Asp114 residue of the neighboring *β*6 subunit can be observed. Although X-ray crystallography provides valuable information about a crystal complex, it is difficult to predict the association state of the covalent inhibitor to the target protein, because the X-ray crystal structure of covalent inhibitor–protein complexes does not always reflect the correct association state.[14] Therefore, a systematic structure–activity relationship study is necessary to confirm whether the interactions observed in the complex structure of covalent inhibitor–protein are crucial in the association state. Our group has investigated a systematic structure–activity relationship of **1** and found that compound **2**, where the ureadipeptide moiety was replaced with an *N*-decanoyl-L-phenylalanine, can exhibit a strong *β*5 subunit inhibitory activity with a K_i' value of 0.14 nM as well as strong cytotoxicity with an IC_{50} value of 2.2 nM against human myeloma RPMI8226 cells.[15] The acyl side chain of **2** plays an important role in improving cell membrane permeability and makes an additional contact with the hydrophobic region of the *β*6 subunit of the 20S proteasome. This additional interaction might have enhanced the inhibitory activity. Of note, the analogue **3**, where the nitrogen at the L-Phe moiety of **2** is methylated, exhibited a large decrease in the *β*5 subunit inhibitory activity (IC_{50} 1000 nM) and completely diminished the cytotoxicity.[16]

* To whom correspondence should be addressed. e-mail: ichikawa@pharm.hokudai.ac.jp

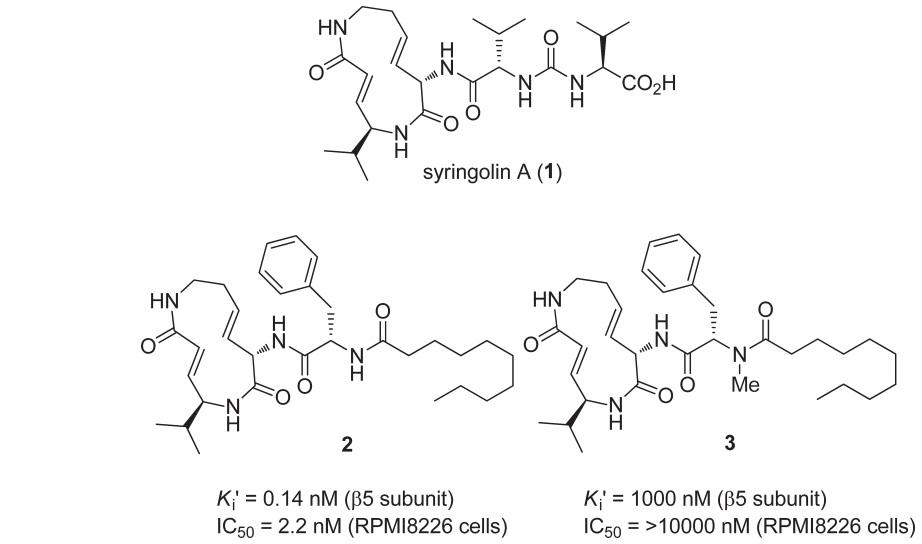

Fig. 1. Structure and Biological Activities of Syringolin A and Its Analogues

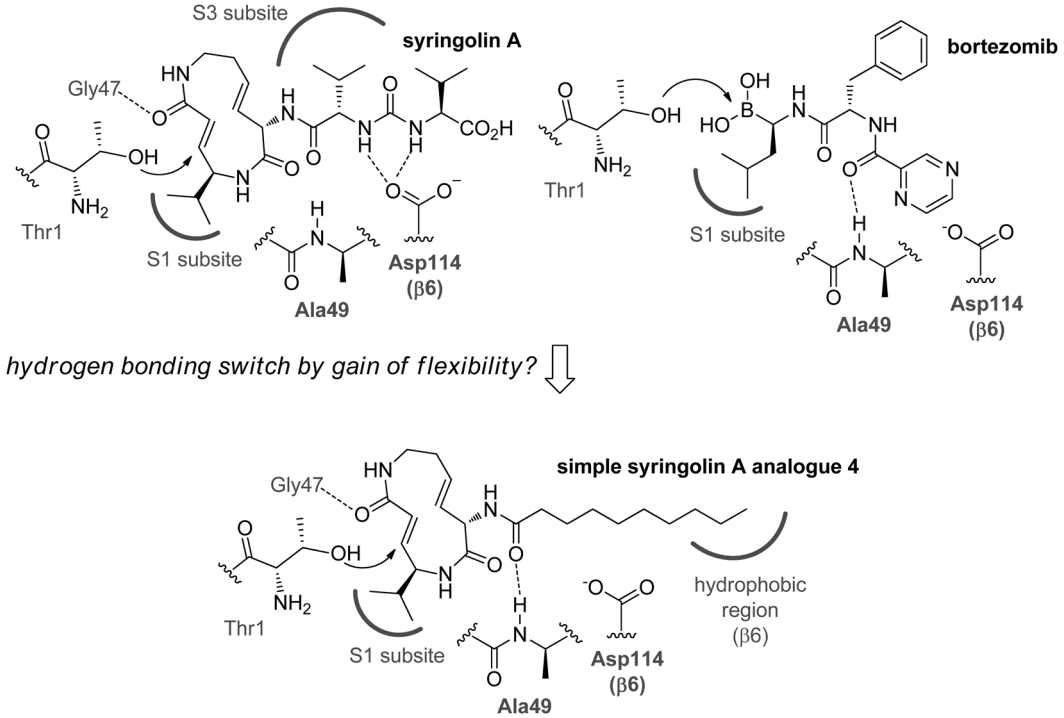

Fig. 2. Expected Binding Mode of Syringolin A and Bortezomib with β5-Subunit of 20S Proteasome and Design of Simplified Analogue by Switching a Key Hydrogen Bonding in Ligand/Target Association

This result indicates that the hydrogen bonding between the NH and the Asp114 of the neighboring β6 residue is a critical interaction between **2** as well as **1** and the β5 subunit in their association state. There exists Ala49 residue near the Asp114 residue in the β6 subunit. In the complex structure of proteasome with bortezomib (PDB code: 2F16), the backbone NH of Ala49 interacts with the carbonyl oxygen of bortezomib (3.23 Å),[17] and it is presumed that the interaction is important in the association state of bortezomib to the β5 subunit. On the other hand, the carbonyl oxygen of internal Val residue of **1** is close to the NH of Ala49, but its distance is 3.63 Å, indicating that the interaction between these functional groups is not likely in the complex with **1**. We hypothesized that removing the substituent recognized by the S3 subsite and the NH group that interact with the Asp114 would increase the flexibility of the side chain. This could induce a reorganization of the structure to switch the hydrogen bonding partners between the oxygen of the exocyclic carboxamide of **1** and the Ala49 of the β5 subunit in the association state. This molecular design allows us to generate a new structurally simplified inhibitor **4**, where the L-phenylalanine residue of **2** is truncated and the acyl side chain is directly attached to the core 12-membered macrolactam. Here, we report the synthesis and biological evaluation of **4** in order to confirm the hypothesis and develop a guide to design new type of syringolin analogues, which are expected to be a next generation proteasome inhibitor.

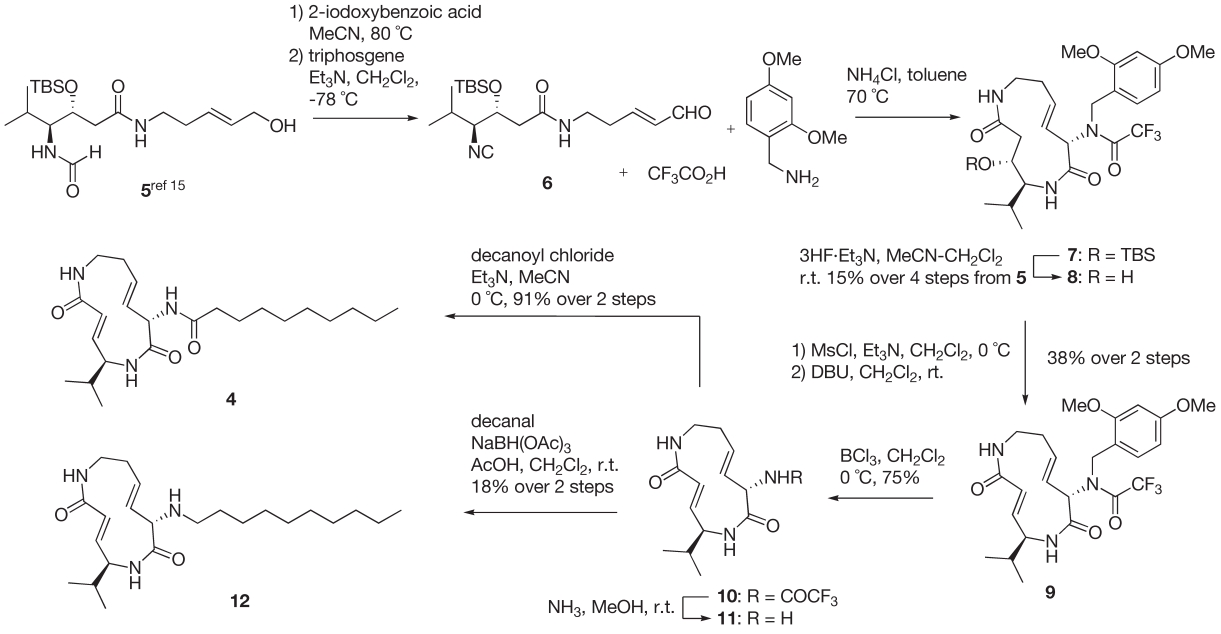

Chart 1. Synthesis of Syringolin A Analogues

Results and Discussion

We have previously reported the total synthesis of **1** featuring intramolecular Ugi-three component reaction with a formylisonitrile, amine, and carboxylic acid.[15] The synthetic strategy was followed for the synthesis of **4** (Chart 1). The known alcohol **5**,[15] which was prepared from *N*-Boc-L-valine in 10 steps, was oxidized by 2-iodoxybenzoic acid (IBX), and the formamide group of the resulting α,β-unsaturated aldehyde was dehydrated by triphosgene in the presence of Et_3N in CH_2Cl_2 at −78°C to provide the formylisonitrile **6**, which was used for the intramolecular Ugi-three component reaction without further purification. The formylisonitrile **6**, 2,4-dimethoxybenzylamine, and trifluoroacetic acid were heated in toluene at 70°C in the presence of NH_4Cl gave the desired 12-membered macrolactam **7**. After removing the *tert*-butyldimethylsilyl (TBS) group of **7** by 3HF–Et_3N in MeCN–CH_2Cl_2, the hydroxylactam **8** was isolated in 15% yield over four steps from **5**. The stereochemistry of the newly formed stereogenic center was found to be in *S*-configuration, and its diastereomer was not detected at all in the reaction mixture. The hydroxyl group of **8** was mesylated and the resulting mesylate was treated with 1,8-diazabicyclo[5.4.0]undec-7-ene (DBU) to promote β-elimination to afford the *E*-α,β-unsaturated carboxamide **9** selectively. The 2,4-dimethoxybenzyl group at the exocyclic nitrogen of **9** was removed by BCl_3 in CH_2Cl_2 at 0°C gave **10** in 75% yield. Next, an acyl side chain was introduced into the 12-membered maclolactam. The acyl side chain is found to be important in increasing the inhibitory activity, presumably by interacting with the β6 subunit of the 20S proteasome (Fig. 2). The length of the acyl side has been optimized by our group, revealing that C8–11 acyl groups were favored and the difference in the biological property among these analogues was very subtle.[16] Thus, a decanoyl group was chosen as the acyl substituent. The trifluoroacetyl group of **10** was removed by saturated NH_3 in MeOH, and the liberated amine **11** was acylated with decanoyl chloride to afford the target analogue **4** in 91% yield over two steps. In order to study the impact of the carbonyl oxygen as a hydrogen acceptor on the inhibitory effect, the *N*-decyl analogue **12**, which lacks a carbonyl oxygen at the side chain, was designed. This was prepared by the reductive alkylation of **11** with decanal in the presence of $NaBH(OAc)_3$ and AcOH in CH_2Cl_2 in 18% yield over two steps from **11**.

For the evaluation of biological activity of the synthesized analogues, the proteasome inhibitor bortezomib was used as a positive control. Compound **4** exhibited much stronger inhibitory activity than the parent natural product **1** with an IC_{50} value of 107 nM. Its inhibitory activity was 9.3 fold stronger than that of **3** (1000 nM). The improved activity of **4** may be due to the switching of a hydrogen bond inside the binding pocket of the β5 subunit. The lack of an NH group in **4** that interacts with the Asp114 residue would allow the oxygen of the exocyclic carboxamide to interact with the Ala49 residue in the association state (Fig. 2). The hydrogen bond switching together with the simplified structure of **4** would form a strong complex between **4** and proteasome. This kind of information may not be obtained from a crystal structure of the covalent complex because the X-ray crystal structure does not always provide structural information that is amenable to the structure-based approach. To form a covalent complex, a covalent inhibitor first associates with its target protein *via* noncovalent interactions to form an inhibitor–protein complex. The chemical reaction then takes place between the inhibitor and the protein to form a covalent complex with a conformational change in the complex. Finally, the conformation of the covalent complex re-organizes to attain an energetically stable state. Therefore, the X-ray crystal structure of covalent inhibitor–protein complexes does not always reflect the association state. The existence of the interaction between the oxygen of the exocyclic carboxamide of **4** and the Ala49 of the β5 subunit in the association state was supported by the fact that analogue **12**, which lacks the carbonyl oxygen that is present at the side chain of **4**, exhibited large decrease in the inhibitory activity showing only 23% inhibition of the β5 proteasome activity at 1000 nM. The trifluoroacetate **10**, which lacks the lipophilic side chain, completely diminished the inhibitory

Table 1. Biological Activities of Syringolin A Analogues

Compound	IC_{50} (nM)[a]	GI_{50} (nM)			
		A431[b]	HCT-116[c]	RKO[c]	RPMI8226[d]
Bortezomib	—	28.2	27	20.8	14.4
Syringolin A (**1**)	680	3240	2830	n.d.[e]	1160
3	10000	>10000	>10000	>10000	>10000
4	107	254	166	109	124
10	>1000	>10000	>10000	>10000	>10000
12	23% Inhibition at 1000 nM	3913	7290	7502	6381

a) Chymotrypsin-like activity of 20S proteasome. *b*) Human epidermal cancer cells. *c*) Human colon cancer cells. *d*) Human myeloma cells. *e*) Not determined.

activity. This indicates the lipophilic side chain attributes to interact with the hydrophobic region of the β6 subunit of the 20S proteasome and this additional interaction plays an important role in enhancement of the inhibitory activity.

Cytotoxicity against a range of human cancer cells including epidermal (A431), colon (HCT-116 and RKO), and myeloma (RPMI8226) cancer cells was also evaluated (Table 1). Overall, the cytotoxicity of the analogues is quite in accordance with the β5 proteasome inhibitory activity. **4** exhibited a potent cytotoxicity against all cells tested in this study with the 50% growth inhibitory concentration (GI_{50}) value of 254 nM for A431, 166 nM for HCT-116, 109 nM for RKO and 124 nM for RPMI8226. Although these values are higher than those of **2**, **4** still exhibited a submicromolar cytotoxicity. There was a large decrease in the cytotoxicity (15–69 fold) in the case of **12** indicating the importance of exocyclic carbonyl moiety. The trifluoroacetate **10** was also tested, however it did not show any cytotoxicity, presumably because the short acyl group did not interact with the β6 subunit and **10** has poor cell membrane permeability.

Conclusion

We designed and synthesized a structurally simplified syringolin A analogue **4**, which could interact with the β5 subunit of 20S proteasome through a switched hydrogen bonding. This analogue exhibits potent inhibitory activity (IC_{50} 107 nM) as well as cytotoxicity against a range human cancer cells at a submicromolar level (109–254 nM). The chemical structure of **4** is very simple compared to the parent natural product with lower molecular weight and the number of chiral center. This analogue is expected to be a promising lead compound and further optimization of **4** would generate a next generation proteasome inhibitor.

Experimental

(4*R*,5*S*,8*S*,9*E*)-1,6-Diaza-8-[*N*-(2,4-dimethoxybenzyl)-*N*-trifluoroacetyl]amino-4-hydroxy-5-isopropyl-2,7-dioxocyclododec-9-en (8) A solution of **5**[15] (2.23 g, 5.76 mmol) in MeCN (58 mL) was treated with IBX (3.23 g, 11.5 mmol) at room temperature, and the mixture was stirred at 80°C for 1 h. The mixture was cooled to 0°C, the insolubles were filtered off through a Celite pad, and the filtrate was concentrated *in vacuo* to afford crude aldehyde. A solution of the crude aldehyde and Et_3N (2.79 mL, 20.2 mmol) in CH_2Cl_2 (58 mL) was treated with triphosgene (855 mg, 2.88 mmol) at −78°C for 30 min. The mixture was quenched with MeOH and partitioned between AcOEt and saturated aqueous $NaHCO_3$. The organic phase was washed with water and brine, dried (Na_2SO_4) and concentrated *in vacuo* to afford a crude isonitrile **6**. A mixture of the crude isonitrile **6**, 2,4-dimethoxybenzylamine (1.73 mL, 11.5 mmol), NH_4Cl (3.08 g, 57.6 mmol) and trifluoroacetic acid (856 μg, 11.5 mmol) in toluene (5.8 L) was stirred at 50°C for 24 h. The whole mixture was concentrated *in vacuo*. The residue was partitioned between AcOEt and 1 M aqueous HCl. The organic phase was washed with saturated aqueous $NaHCO_3$, water and brine, dried (Na_2SO_4), filtered, and concentrated *in vacuo* to afford Ugi-product **7** as a yellow oil. A solution of the Ugi-product in MeCN–CH_2Cl_2 (1 : 1) (58 mL) was treated with $3HF \cdot Et_3N$ (9.4 mL, 57.6 mmol) at room temperature for 2 d. The reaction mixture was partitioned between AcOEt and saturated aqueous $NaHCO_3$. The organic phase was washed with water and brine, dried (Na_2SO_4), filtered, and concentrated *in vacuo*. The residue was purified by column chromatography (2% MeOH–$CHCl_3$) to afford **8** (436 mg, 15%) as a yellow oil. ^{1}H-NMR ($CDCl_3$, 400 MHz, a mixture several rotamers at 20°C) Selected data for the major rotamer δ: 7.13 (d, 1H, Ph-H, J=8.2 Hz), 6.40 (m, 2H, Ph-H), 6.27 (d, 1H, NH, J=7.3 Hz), 5.65 (m, 2H, H-9, 10), 5.50 (m, 1H, NH), 4.83–4.52 (m, 3H, H-8, Bn), 4.21 (m, 1H, H-5), 3.92–3.69 (m, 8H, H-12, OMe), 2.83 (br s, 1H, H-4), 2.52 (m, 2H, H-11), 2.19 (d, 1H, H-3, J=12.8 Hz), 2.12 (m, 1H, H-1′), 1.91 (m, 1H, H-3), 1.01–0.70 (m, 6H, Me); ^{13}C-NMR ($CDCl_3$, 100 MHz) δ: 173.2, 169.9, 160.7 (d, $J_{F,C}$=43.9 Hz), 158.8, 157.4, 135.7, 128.9, 125.6, 123.6 (d, $J_{F,C}$=347.8 Hz), 116.6, 104.1, 98.2, 69.2, 68.5, 65.5, 60.3, 55.5, 45.3, 40.0, 37.5, 34.6, 29.7, 20.0, 19.0; low resolution-electrospray ionization (LR-ESI)-MS m/z 538 [(M+Na)$^+$]; high resolution (HR)-ESI-MS Calcd for $C_{24}H_{32}F_3N_3NaO_6$ 538.2141. Found 538.2135.

(4*R*,5*S*,8*S*,9*E*)-1,6-Diaza-8-[*N*-(2,4-dimethoxybenzyl)-trifluoroacetamido-5-isopropyl-2,7-dioxocyclododeca-3,9-diene (9) A solution of **8** (290 mg, 0.40 mmol) and Et_3N (333 μL, 2.40 mmol) in CH_2Cl_2 (4 mL) was treated with MsCl (93.0 μL, 1.20 mmol) at 0°C for 10 min. The mixture was partitioned between AcOEt and 1 M aqueous HCl. The organic phase was washed with saturated aqueous $NaHCO_3$, water and brine, dried (Na_2SO_4), filtered, and concentrated *in vacuo* to afford crude mesylate. A solution of the crude mesylate in CH_2Cl_2 (4 mL) was treated with DBU (359 μL, 2.40 mmol) at room temperature for 2 d. The mixture was partitioned between AcOEt and 1 M aqueous HCl. The organic phase was washed with saturated aqueous $NaHCO_3$, water and brine, dried (Na_2SO_4), filtered, and concentrated *in vacuo*. The residue was purified by column chromatography (3% MeOH–$CHCl_3$) to afford **9** (105 mg, 38%) as a colorless

solid. ^{1}H-NMR (DMSO-d_6, 400 MHz, a mixture several rotamers at 20°C). Selected data for the major rotamer δ: 8.27 (d, 1H, NH, $J_{N,5}$=7.8 Hz), 7.49 (m, 1H, NH), 7.05 (d, 1H, Ph-H, J=8.7 Hz), 6.70 (dd, 1H, H-4, $J_{4,5}$=5.0, $J_{4,3}$=15.6 Hz), 6.45 (brs, 2H, Ph-H), 6.08 (d, 1H, H-3, $J_{3,4}$=15.6 Hz), 5.49 (m, 1H, H-10), 5.23 (d, 1H, H-8, $J_{8,9}$=7.8 Hz), 5.10 (dd, 1H, H-9, $J_{9,8}$=7.8, $J_{9,10}$=15.6 Hz), 4.72–4.40 (m, 2H, PhCH$_2$), 4.12 (brs, 1H, H-5), 3.73 (s, 6H, OMe), 3.13 (brs, 1H, H-12), 3.03 (brs, 1H, H-12), 2.02–1.64 (m, 2H, H-11), 1.73 (dt, 1H, H-1′, $J_{1',Me}$=6.9, $J_{1',5}$=14.2 Hz), 0.90 (d, 6H, Me, $J_{Me,1'}$=6.9 Hz); ^{13}C-NMR (DMSO-d_6, 100 MHz) δ: 168.2, 166.1, 159.3, 156.0 (d, $J_{F,C}$=40.2 Hz), 143.2, 137.3, 127.3, 126.3, 121.6, 121.0, 119.5 (d, $J_{F,C}$=369.8 Hz), 117.7, 104.4, 97.9, 60.2, 55.4, 55.1, 43.2, 42.6, 35.2, 31.6, 19.8, 19.4, 19.2; LR-ESI-MS m/z 520 [(M+Na)$^+$]; HR-ESI-MS Calcd for $C_{24}H_{30}F_3N_3NaO_5$ 520.2035. Found 520.2030; $[\alpha]_D^{20}$ −62.9 (c=0.48, dimethyl sulfoxide (DMSO)).

(4*R*,5*S*,8*S*,9*E*)-1,6-Diaza-8-trifluoroacetamido-5-isopropyl-2,7-dioxocyclododeca-3,9-diene (10) A solution of **9** (162 mg, 0.31 mmol) in CH_2Cl_2 (10 mL) was treated with BCl_3 (1 M CH_2Cl_2 solution) (3.10 mL, 3.10 mmol) at 0°C for 2 h. The mixture was partitioned between AcOEt and saturated aqueous $NaHCO_3$. The organic phase was washed with water and brine, dried (Na_2SO_4), filtrated, and concentrated *in vacuo*. The residue was purified by column chromatography (3% MeOH–$CHCl_3$) to afford **10** (80.6 mg, 75%) as a colorless solid. ^{1}H-NMR (DMSO-d_6, 400 MHz) δ: 9.75 (d, 1H, NH, $J_{NH,8}$=6.2 Hz), 8.19 (d, 1H, NH, $J_{NH,5}$=6.9 Hz), 7.50 (t, 1H, NH, $J_{NH,12}$=7.1 Hz), 6.69 (dd, 1H, H-4, $J_{4,5}$=6.9, $J_{4,3}$=15.6 Hz), 6.08 (d, 1H, H-3, $J_{3,4}$=15.6 Hz), 5.72 (dt, 1H, H-10, $J_{10,11}$=7.8, $J_{10,9}$=15.8 Hz), 5.46 (dd, 1H, H-9, $J_{9,8}$=6.2, $J_{9,10}$=15.8 Hz), 4.92 (t, 1H, H-8, $J_{8,9}$=$J_{8,NH}$=6.2 Hz), 4.08 (dt, 1H, H-5, $J_{5,4}$=$J_{5,NH}$=6.9, $J_{5,1'}$=14.2 Hz), 3.18 (m, 2H, H-12), 2.32 (m, 1H, H-11), 1.97 (m, 1H, H-11), 1.73 (dt, 1H, H-1′, $J_{1',Me}$=7.0, $J_{1',5}$=14.2 Hz), 0.94 (d, 3H, Me, $J_{Me,1'}$=7.0 Hz), 0.90 (d, 3H, Me, $J_{Me,1'}$=7.0 Hz); ^{13}C-NMR ($CDCl_3$, 100 MHz) δ: 167.9, 166.2, 156.1 (d, $J_{F,C}$=36.4 Hz), 143.3, 134.9, 123.6, 121.6, 115.8 (d, $J_{F,C}$=289.3 Hz), 55.6, 54.8, 42.3, 35.2, 31.5, 19.7, 19.2; LR-ESI-MS m/z 370 [(M+Na)$^+$]; HR-ESI-MS Calcd for $C_{15}H_{20}F_3N_3NaO_3Si$ 370.1354. Found 370.1349.

(4*R*,5*S*,8*S*,9*E*)-1,6-Diaza-8-decanamido-5-isopropyl-2,7-dioxocyclododeca-3,9-diene (4) Compound **10** (5.5 mg, 15.8 μmol) was treated with saturated ammonia in methanol solution (1 mL) at room temperature for 13 h. The mixture was concentrated *in vacuo* to afford crude amine **11**. A solution of the crude amine and Et_3N (6.6 μL, 47.4 μmol) in MeCN (1 mL) was treated with decanoyl chloride (3.8 μL, 19.0 μmol) at 0°C for 10 min. The mixture was partitioned between AcOEt and 1 M aqueous HCl. The organic phase was washed with saturated aqueous $NaHCO_3$, water and brine, dried (Na_2SO_4), filtered, and concentrated *in vacuo*. The residue was purified by column chromatography (3% MeOH–$CHCl_3$) to afford **4** (5.8 mg, 91%) as a white solid. ^{1}H-NMR (CD_3OD, 400 MHz) δ: 6.96 (dd, 1H, H-4, $J_{4,5}$=4.8, $J_{4,3}$=15.7 Hz), 6.21 (d, 1H, H-3, $J_{3,4}$=15.7 Hz), 5.64 (m, 2H, H-9, 10), 4,18 (brs, 1H, H-8), 3.43–3.18 (m, 2H, H-12), 2.32 (brs, 1H, H-11), 2.22 (brs, 3H, H-11, H-2″), 1.82 (m, 1H, H-1′), 1.59 (brs, 2H, H-13″), 1.40–1.21 (brs, 12H, CH$_2$), 1.06 (d, 3H, Me, J=6.4 Hz), 1.01 (d, 3H, Me, J=8.1 Hz), 0.89 (s, 3H, Me); ^{13}C-NMR was not able to be analyzed because of the solubility of the compound; LR-ESI-MS m/z 428 [(M+Na)$^+$]; HR-ESI-MS Calcd for $C_{23}H_{39}N_3NaO_3$ 428.2889. Found 428.2873.

(4*R*,5*S*,8*S*,9*E*)-1,6-Diaza-8-(1-decyl)amino-5-isopropyl-2,7-dioxocyclododeca-3,9-diene (12) Compound **10** (10.0 mg, 28.8 μmol) was treated with saturated ammonia in methanol solution (2 mL) at room temperature for 13 h. The mixture was concentrated *in vacuo* to afford crude amine **11**. A mixture of the crude amine, decanal (5.4 μL, 28.8 μmol) and AcOH (8.2 μL, 144 μmol) in MeCN (1 mL) was stirred at room temperature for 10 min. $NaBH(OAc)_3$ (12.0 mg, 57.6 μmol) was added to the mixture and stirred at room temperature for 1 d. Decanal (2.7 μL, 14.4 μmol) and $NaBH(OAc)_3$ (6.0 mg, 28.8 μmol) was added to the mixture and stirred at room temperature for 1 d. The reaction was quenched with saturated aqueous $NaHCO_3$ and the organic phase was washed with water and brine, dried (Na_2SO_4), filtered, and concentrated *in vacuo*. The residue was purified by column chromatography (4% MeOH–$CHCl_3$) to afford **12** (2.0 mg, 18%) as a white solid. ^{1}H-NMR (DMSO-d_6, 400 MHz) δ: 7.88 (d, 1H, NH, $J_{NH,5}$=7.4 Hz), 7.44 (t, 1H, NH, $J_{NH,12}$=7.1 Hz), 6.67 (dd, 1H, H-4, $J_{4,5}$=7.3, $J_{4,3}$=15.4 Hz), 6.08 (d, 1H, H-3, $J_{3,4}$=15.4 Hz), 5.46 (dt, 1H, H-10, $J_{10,11}$=7.3, $J_{10,9}$=16.4 Hz), 5.27 (dd, 1H, H-9, $J_{9,8}$=7.5, $J_{9,10}$=16.4 Hz), 4.09 (brs, 1H, H-5), 3.70 (d, 1H, H-8, $J_{8,9}$=7.5 Hz), 3.14 (m, 2H, H-12), 2.45–2.29 (m, 2H, H-1″), 2.22 (brs, 1H, H-11), 1.96 (brs, 1H, H-11), 1.74 (brs, 1H, H-1′), 1.34 (brs, 1H, NH), 1.23 (m, 16H, CH$_2$), 0.97–0.81 (m, 9H, Me); ^{13}C-NMR (DMSO-d_6, 125 MHz) δ: 166.4, 143.3, 131.4, 125.1, 120.7, 111.8, 55.5, 55.4, 47.2, 42.7, 35.1, 31.3, 29.6, 29.6, 29.0, 28.8, 28.7, 26.8, 22.1, 19.8, 19.8, 19.3, 14.0; LR-ESI-MS m/z 414 [(M+Na)$^+$]; HR-ESI-MS Calcd for $C_{23}H_{41}N_3NaO_2$ 414.3096. Found 414.3091; $[\alpha]_D^{23}$ +27.8 (c=0.10, DMSO).

Evaluation of *in Vitro* Chymotrypsin-Like (CT-L) Activity of 20S Proteasome *In vitro* proteasome assays were performed in 96-wel microtiter plates with human erythrocyte 20S proteasome (R&D Systems, Inc.) using the AK-740 Assay Kit for Drug Discovery (Biomol). Reactions were performed at 37°C in 100 μL volumes containing a serial dilution of test samples, 2 μg/mL 20S proteasome, and 100 μM Suc-LLVY-AMC for assaying chymotrypsin-like activity, according to the manufacturer's instructions. Fluorescence was monitored with infinite M200 microplate reader (Tecan) equipped with 360 nm excitation and 465 nm emission filters.

Measurement of Cytotoxicity Antiproliferative activities of the compounds against A431, HCT-116, RKO, TOV21G, CCRF-CEM, RPMI8226 cells were measured by quantifying the amount of ATP as follows. Briefly, cells (1–2×10^3 cells/well) in a 96 well plate were cultured in RPMI medium containing 10% fetal bovine serum in the presence of test compounds at 37°C for 72 h under 5% CO_2 atmosphere. Then, a solution of CA-1000 reagents (TOYO INK Co., Ltd.) was added, and plates were shaken and luminescence of oxyluciferin was monitored with the plates held at 23°C.

Acknowledgments We thank Ms. S. Oka and Ms. A. Tokumitsu (Center for Instrumental Analysis, Hokkaido University) for the measurement of mass spectra. This research was supported by JSPS Grant-in-Aid for Challenging Exploratory Research (SI, Grant Number 22659020), Scientific Research (B) (SI, Grant Number 25293026), Scientific Research on Innovative Areas "Chemical Biology of Natural Products" (SI, Grant Number 24102502).

Conflict of Interest The authors declare no conflict of

interest.

References

1) Bross P. F., Kane R., Farrell A. T., Abraham S., Benson K., Brower M. E., Bradley S., Gobburu J. V., Goheer A., Lee S.-L., Leighton J., Liang C. Y., Lostritto R. T., McGuinn W. D., Morse D. E., Rahman A., Rosario L. A., Verbois S. L., Williams G., Wang Y.-C., Pazdur R., *Clin. Cancer Res.*, **10**, 3954–3964 (2004).
2) Herndon T. M., Deisseroth A., Kaminskas E., Kane R. C., Koti K. M., Rothmann M. D., Habtemariam B., Bullock J., Bray J. D., Hawes J., Palmby T. R., Jee J., Adams W., Mahayni H., Brown J., Dorantes A., Sridhara R., Farrell A. T., Pazdur R., *Clin. Cancer Res.*, **19**, 4559–4563 (2013).
3) Kisselev A. F., van der Linden W. A., Overkleeft H. S., *Chem. Biol.*, **19**, 99–115 (2012).
4) Murata S., Yashiroda H., Tanaka K., *Nat. Rev. Mol. Cell Biol.*, **10**, 104–115 (2009).
5) Lü S., Wang J., *Biomarker Res.*, **1**, 13 (2013).
6) Alsina M., Trudel S., Furman R. R., Rosen P. J., O'Connor O. A., Comenzo R. L., Wong A., Kunkel L. A., Molineaux C. J., Goy A., *Clin. Cancer Res.*, **18**, 4830–4840 (2012).
7) Wäspi U., Blanc D., Winkler T., Rüedi P., Dudler R., *Mol. Plant Microbe Interact.*, **11**, 727–733 (1998).
8) Gröll M., Schellenberg B., Bachmann A. S., Archer C. R., Huber R., Powell T. K., Lindow S., Kaiser M., Dudler R., *Nature* (London), **452**, 755–758 (2008).
9) Clerc J., Groll M., Illich D. J., Bachmann A. S., Huber R., Schellenberg B., Dudler R., Kaiser M., *Proc. Natl. Acad. Sci. U.S.A.*, **106**, 6507–6512 (2009).
10) Clerc J., Schellenberg B., Gröll M., Bachmann A. S., Huber R., Dudler R., Kaiser M., *Eur. J. Org. Chem.*, **2010**, 3991–4003 (2010).
11) Clerc J., Li N., Krahn D., Groll M., Bachmann A. S., Florea B. I., Overkleeft H. S., Kaiser M., *Chem. Commun.*, **47**, 385–387 (2011).
12) Archer C. R., Groll M., Stein M. L., Schellenberg B., Clerc J., Kaiser M., Kondratyuk T. P., Pezzuto J. M., Dudler R., Bachmann A. S., *Biochemistry*, **51**, 6880–6888 (2012).
13) Totaro K. A., Barthelme D. B., Simpson P. T., Sauer R. T., Sello J. K., *Bioorg. Med. Chem.*, **23**, 6218–6222 (2015).
14) Kawamura S., Unno Y., Tanaka M., Sasaki T., Yamano A., Hirokawa T., Kameda T., Asai A., Arisawa M., Shuto S., *J. Med. Chem.*, **56**, 5829–5842 (2013).
15) Chiba T., Hosono H., Nakagawa K., Asaka M., Takeda H., Matsuda A., Ichikawa S., *Angew. Chem. Int. Ed.*, **53**, 4836–4839 (2014).
16) Chiba T., Matsuda A., Ichikawa S., *Bioorg. Med. Chem. Lett.*, **25**, 4872–4877 (2015).
17) Gröll M., Berkers C. R., Ploegh H. L., Ovaa H., *Structure*, **14**, 451–456 (2006).